Clustering in Cu-Ni alloys: A diffuse neutron-scattering study

J. Vrijen
Netherlands Energy Research Foundation ECN, Petten, The Netherlands

S. Radelaar
Physics Laboratory, Rijksuniversiteit Utrecht, Utrecht, The Netherlands

(Received 24 August 1977)

Clustering in Cu-Ni was measured from the diffuse scattering of thermal neutrons, using the special isotopes ^{62}Ni and ^{65}Cu for optimizing scattering conditions. Both the temperature and the composition dependence of clustering have been studied systematically. Alloys with compositions ranging from 20- to 80-at.% Ni were investigated in equilibrium for temperatures between 400 and 700°C. The cluster parameters show a strong asymmetry in their composition dependence. This asymmetry appears to be temperature dependent. The results show that many-particle interactions play an important role in determining the amount of clustering in Cu-Ni. The location of the miscibility gap is calculated.

INTRODUCTION

Fairly much is known about the preference for unlike atoms as nearest neighbors in the homogeneous phase of binary alloys, which is generally known as short-range order (SRO). The Cu-Au system with its three ordered structures Cu_3Au, CuAu, and $CuAu_3$ has been investigated most intensively.[1-4] An increasing amount of often very detailed and accurate SRO data made it possible to test various statistical theories. Most of these[5-10] are based on the assumption that SRO and clustering (preference for like nearest neighbors) can be described with pairwise interactions only. It is probably more realistic to consider also many-particle interactions as in the cluster variation method of Kikuchi.[11] This can result in a correct description of the transition temperature as a function of the composition as was shown by Van Baal[12] for Cu-Au. The two types of models should be considered as complementary.

Much less is known about clustering. Due to the specific distribution of the intensity of diffuse scattering around fundamental reflections it is much more complicated to measure clustering even in systems comparable otherwise. An attractive candidate for investigating clustering is Cu-Ni, since it is a relatively simple system: (i) The lattice parameters of the pure elements differ very little and thus no large elastic strains will be induced by clustering. (ii) Complete solid solubility exists over a wide temperature range. (iii) Equilibrium states of the system can be reached in an accessible temperature region. (iv) It is one of the systems most suited for diffuse-scattering experiments, when measured with thermal neutrons in combination with the use of the isotopes ^{62}Ni and ^{65}Cu, as will be explained later.

Meijering[13] was one of the first who predicted clustering in Cu-Ni. His work as well as most of the later investigations[14-20] was concerned only with the miscibility gap. Only a few quantitative neutron experiments dealing with clustering have been published.[21-24] The Warren-Cowley cluster parameters derived from these scattering experiments have been collected in Table I. Also NMR measurements have produced clustering data,[25] but the assumptions necessary for deducing these data make them much less accurate than those from scattering experiments. Unfortunately, in all these investigations very little attention has been given to the heat treatment of the samples. Probably this is one of the sources of error which cause the discrepancies between the reported data. These discrepancies are large and not in agreement with the experimental uncertainties given, not even for α_1. In a study of clustering in Cu-Ni careful and well-defined heat treatments are of crucial importance for obtaining reliable and consistent data. Therefore, we systematically studied the composition and temperature dependence of clustering in this system by means of diffuse scattering of thermal neutrons. For optimal experimental results ^{62}Ni and ^{65}Cu have been used. In order to avoid misinterpretations only reproducible atomic distributions have been investigated, quenched from thermal equilibrium at various temperatures. Therefore, also the essentials of specimen preparation, heat treatments, and the data reduction have been given in detail.

EXPERIMENTAL METHOD

The differential cross section for the elastic scattering of thermal neutrons from a binary solid system with only short-range correlations between the occupation of the sites can be written[21,26]

TABLE I. First four Warren-Cowley cluster parameters together with the sample specifications for Cu-Ni alloys from investigations reported in the literature (Refs. 21–24). All data have been measured by diffuse neutron scattering from polycrystalline samples. Some of these samples were isotopically enriched. The resolution in real space is also given, due to the limited range of the investigated reciprocal space.

at.% Ni	Specimen size	Specifications heat treatment	α_1 $r_1 \approx 2.5$ Å	α_2 $r_2 \approx 3.5$ Å	α_3 $r_3 \approx 4.3$ Å	α_4 $R_4 \approx 5.0$ Å	κ range ($Å^{-1}$)	Resolution real space (Å)	Reference
90	slab, 6-mm thickness	3 d 1000 °C quenched	0.055(10)	0.048(15)	−0.005(7)	0.004(10)	0.3–1.1	3.45	23
80	slab, 6-mm thickness	3 d 1000 °C quenched	0.080(4)	0.062(7)	−0.007(3)	0.007(4)	0.3–1.1	3.45	23
80 ^{60}Ni	cylinder 9 × 60 mm	24 h 1000 °C quenched	0.046(2)	0.039(8)	−0.010(3)	0.020(6)	0.6–2.5	1.52	22
80.2 ^{62}Ni	slab, 1.5-mm thickness	16 h 1050 °C quenched	0.1175(35)	−0.0614	0.0445	−0.0584	0.3–2.5	1.52	24
70	slab, 6-mm thickness	3 d 1000 °C quenched	0.118(2)	0.053(5)	−0.001(1)	0.009(2)	0.2–1.1	3.45	23
70.4 ^{62}Ni	slab, 1.5-mm thickness	16 h 1050 °C quenched	0.1432(82)	−0.0328	0.0432	−0.0098	0.3–2.5	1.52	24
60	slab, 6-mm thickness	3 d 1000 °C quenched	0.103(3)	−0.001(6)	0.009(2)	0.009(3)	0.2–1.1	3.45	23
50	slab, 6-mm thickness	3 d 1000 °C quenched	0.106(2)	−0.009(4)	0.008(1)	0.007(2)	0.2–0.8	4.75	23
47.5 ^{62}Ni	slab, 1.5-mm thickness	16 h 1050 °C quenched	0.1335(33)	−0.0747	0.0436	−0.0479	0.3–2.5	1.52	24
47.5 ^{62}Ni	slab, 1.8-mm thickness	furnace cooled 450–550 °C	0.1210	−0.0083	0.0103	0.0098	0.2–8.8	0.43	21

$$\frac{d\sigma}{d\Omega} = Nc_A c_B (b_A - b_B)^2 \sum_n (\alpha_n + \beta_n i\vec{\kappa}\cdot\vec{r}_n) e^{i\vec{\kappa}\cdot\vec{r}_n} + (c_A b_A + c_B b_B)^2 \sum_n \sum_{n'} e^{i\vec{\kappa}\cdot(\vec{r}_n - \vec{r}_{n'})} \quad (1)$$

analogous to that for x-ray scattering.[27] N is the number of lattice sites in the system, c_A and c_B are the atomic fractions of the components A and B, b_A and b_B their effective scattering lengths, α_n the Warren-Cowley SRO parameters, $\vec{\kappa}$ the scattering vector, and $\vec{r}_n$ the position vector of site n. β_n is the size-effect parameter, defined by

$$\beta_n = \frac{b_B}{b_B - b_A} \epsilon_n^{BB} \left(\frac{c_B}{c_A} + \alpha_n\right) - \frac{b_A}{b_B - b_A} \epsilon_n^{AA} \left(\frac{c_A}{c_B} + \alpha_n\right), \quad (2)$$

where ϵ_n^{BB} and ϵ_n^{AA} are the average fractional changes in the average interatomic distance r_n when the pairs are BB or AA, respectively. For simplicity the Debye-Waller factors and the other usual contributions to the differential scattering cross section, e.g., isotopic incoherent, spin incoherent, multiple and magnetic scattering, have been omitted in Eq. (1). These contributions will be discussed later in more detail. The second term on the right-hand side of Eq. (1) describes the fundamental Bragg reflections of the lattice with atoms with an average scattering length of $(c_A b_A + c_B b_B)$. The first term describes the diffuse scattering and it will be clear that for optimal observability the factor $(b_A - b_B)^2$ should be as large as possible. The use of ^{62}Ni ($b_{^{62}\mathrm{Ni}} = -0.87\times10^{-12}$ cm) together with ^{65}Cu ($b_{^{65}\mathrm{Cu}} = 1.11\times10^{-12}$ cm) instead of natural Ni ($\bar{b}_{\mathrm{Ni}} = 1.03\times10^{-12}$ cm) and Cu ($\bar{b}_{\mathrm{Cu}} = 0.76\times10^{-12}$ cm) increases this factor drastically. This is illustrated by Fig. 1, where the partial cross sections for the Bragg, diffuse, and incoherent scattering are given as a function of composition for the natural Cu-Ni alloys and for the alloys enriched in ^{65}Cu and ^{62}Ni. Since $b_{^{62}\mathrm{Ni}}$ is negative a composition can be made, the so called null matrix, with $(c_A b_A + c_B b_B)^2 = 0$, which implies that for that composition ($^{62}\mathrm{Ni}_{0.565}{}^{65}\mathrm{Cu}_{0.435}$) all Bragg scattering vanishes. Moreover, the choice of isotopes of a purity as specified later reduces the background due to isotopic incoherence to very low values. All samples were polycrystalline. For polycrystalline cubic alloys the diffuse part of Eq. (1) becomes

$$\left(\frac{d\sigma}{d\Omega}\right)_{\mathrm{diff}} = Nc_A c_B (b_A - b_B)^2 \times \sum_i C_i \left((\alpha_i - \beta_i)\frac{\sin\kappa r_i}{\kappa r_i} + \beta_i \cos\kappa r_i\right), \quad (3)$$

where C_i is the coordination number for the ith shell.

The neutron diffraction data of all samples have been collected at room temperatures with one of the neutron spectrometers at the reactor HFR at Petten. The neutron wavelength could be changed continuously between $\lambda = 1.1$ Å and $\lambda = 4.0$ Å. Also the distance between specimen and detector could be varied within certain limits. Soller slits with a horizontal divergence of 30 and 40 min and sometimes 20 and 40 min have been used between monochromator and specimen and between speci-

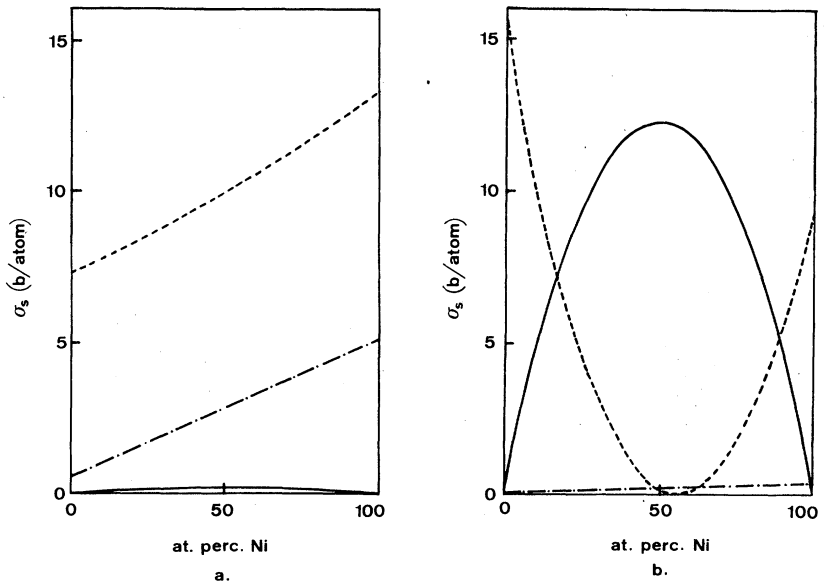

FIG. 1. Bragg (---), diffuse (——), and incoherent (-·-·-) contributions to the cross section for the nuclear scattering of thermal neutrons. Both for natural Cu-Ni (a) and for the isotopically enriched alloys ^{65}Cu-^{62}Ni (b).

men and BF_3 counter, respectively. A focusing pyrolytic graphite monochromator was used to obtain the desired wavelength and, when necessary, a pyrolytic graphite filter was used to restrict higher-order neutrons to less than 1% .[28]

SPECIMEN PREPARATION

The isotopes ^{62}Ni and ^{65}Cu that have been used, were purchased from Oak Ridge National Laboratories (batch 175601, 98.83% ^{62}Ni, and batch 195601, 97.94% ^{62}Ni; major impurities: Ca, Cu, Mg, Si: 100 ppm, Zn < 0.2%, Fe < 200 ppm, and batch 165780, 99.69% ^{65}Cu; major impurities: Zn < 0.2%). The materials were mixed in the appropriate amounts and reduced during 48 h in a hydrogen flow at 900 °C. Thereafter the mixture has been melted under extremely pure He in order to limit the evaporation of Cu and to obtain the necessary heat-conducting atmosphere for fast cooling. Coring could not be avoided entirely by cooling in this way and the distances between the dendrites were 40–60 μm. The ingots have been homogenized by cold rolling and subsequently they were annealed for one week at temperatures between 1050 and 1200 °C, depending on the composition, in an evacuated silica tube. The final form of a nearly circular disk of thickness between 0.9 and 1.2 mm was obtained by cold rolling in various directions. The induced strains have been relieved by annealing for 2 h at 700 °C *in vacuo*. The grain size of the samples typically ranged from 40 to 80 μm and, since roughly 650 mm^3 of the sample was used for the scattering experiments, the specimen consisted of more than 10^5 grains. A texture investigation did not indicate any preferred orientation of these grains. The compositions of the samples were checked with a Perkin Elmer atomic absorption spectrophotometer. The deviations from the nominal compositions appeared to be less than 1 at.% . The reproducibility of the amount of clustering as a function of temperature has been checked by starting all measurements with a low-temperature equilibrium state, followed by the various high-temperature equilibria and finally again a low-temperature equilibrium. The results of the first and last measurements were always in agreement.

After annealing at the desired temperature the specimens were water quenched. Assuming a cooling rate of about 10^4 °C/sec for these samples of about 1 mm thickness and considering the model calculations by Andries *et al.*[29] and the data for clustering kinetics in Cu-Ni of Van Royen *et al.*[30] made quench temperatures above 700 °C unfit for use. This has been checked for the sample with 70-at.% Ni by quenching it also from higher temperatures. From Fig. 2 it is obvious that no really more disordered equilibrium state than that at about 700 °C can be achieved by going to higher quench temperatures. For the more Cu-rich samples with a higher atomic mobility the deviation might occur at a somewhat lower temperature, but not so much lower that 700 °C could not be used.

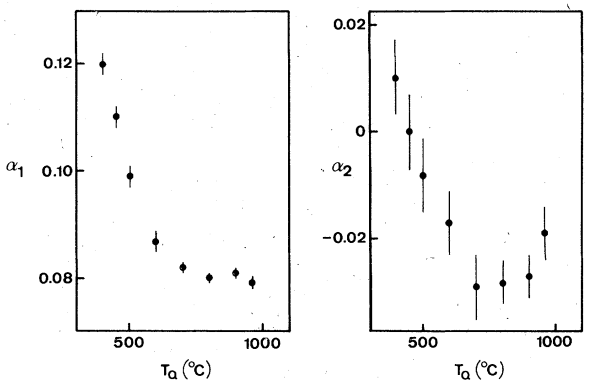

FIG. 2. Effect of the quench temperature on the cluster parameters α_1 and α_2 in $^{65}Cu_{0.30}{}^{62}Ni_{0.70}$ by quenching in water ($\dot{T} \sim 10^4$ °C-sec).

DATA HANDLING

For the data reduction a number of corrections must be applied. One must correct for fast neutrons, for the thermal background and for geometric effects in transmission in a thin flat specimen. The thermal background and fast neutron contributions were very low for the used spectrometer arrangements. In Fig. 3 it can be seen that only at very small angles these contributions become a significant part of the total scattered intensity.

The thermal vibrations of the lattice have been accounted for by taking mean square amplitudes of these vibrations in a Debye model.[29] For the different shells[27] the effective fractions of this mean square amplitude were taken.[21] This mean square amplitude was assumed to be linear in the composition.

In the diffraction experiments no energy analysis of the scattered neutrons was made. Hence the integrated cross section obtained must be corrected for inelastic contributions. This has been done in the incoherent approximation of Placzek,[31] according to the relation

$$\left.\frac{d\sigma}{d\Omega}\right|_{\text{meas}} \simeq \left.\frac{d\sigma}{d\Omega}\right|_{\text{elas}} \left(1 + A - B\,\frac{\kappa^2}{k_0^2}\right) \qquad (4)$$

which has been treated in more detail by Yarnell *et al.*[32] $\vec{k}_0$ is the incident wave vector, A and B are constants, determined by the incident energy of the neutrons, counter efficiency, and the recoil

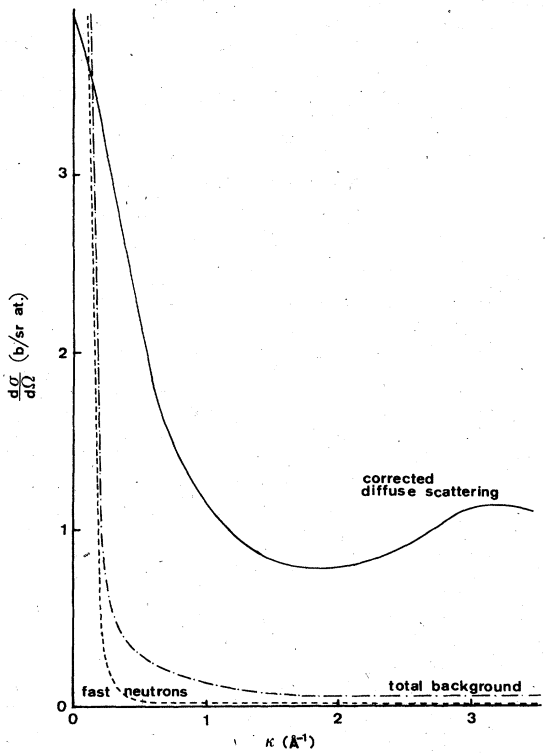

FIG. 3. Typical background contributions to the total scattering, compared with the corrected diffuse scattering pattern of $^{65}Cu_{0.40}{}^{62}Ni_{0.60}$, in equilibrium at 450 °C. The neutron wavelength is 2.58 Å.

energy of the scattering atoms. For vanadium the results of these corrections were satisfactory, since the corrected intensity is independent of the scattering angle within the accuracy of the measurements (counting statistics between 0.1 and 0.5%).

Therefore, the same method has been applied to the Cu-Ni data. The corrections remain very small (a few per cent) for these heavy nuclei. Multiple scattering, was computed following a procedure outlined by Vineyard[33] and Sears.[34] In order to minimize this contribution and its angular dependence thin samples have been used in a symmetric scattering mode. For the used Cu-Ni samples the angular dependence of the multiple fraction was less than 0.3% for $0 < 2\theta \leq 90°$ and therefore it could be neglected. Depending on wavelength, thickness and composition of the samples this fraction varied between 10 and 20% of the primary intensity. The isotopic incoherence is very low in these samples, but not equal to zero (see Fig. 1). Therefore, this contribution has also been corrected for. Spin incoherence does not occur in Cu or in Ni.[35] Para- or ferromagnetic contributions to the cross section have been neglected since they are very small compared to the enhanced nuclear diffuse terms.

In order to cover a sufficiently large-κ range, necessary for a high resolution in real space, neutrons of two different wavelengths, usually $\lambda = 1.16$ Å and $\lambda = 2.58$ Å, were used for an investigation of the null matrix. For joining these two sets of data a procedure of scaling by a numerical integration of the overlapping region has been used, taking into account the differences in the corrections mentioned above. The measurements were put on an absolute scale by comparison with the incoherent scattering of vanadium. Within small uncertainties introduced by the specimen thickness this calibration agreed very well with calculations of the Laue intensity of the samples ($\alpha_0 = 1.00 \pm 0.03$).

Finally a least-squares fit of Eq. (3) to the data, weighted with their statistical error resulted in a set of cluster parameters α_i. The fit consisted of a repeating series, at every step increasing the number of shells with one. In this way the convergence of the fit procedure could be followed. Taking too many separate shell parameters, which means exceeding the spatial resolution determined by the investigated κ range, resulted in nonphysical oscillations in the values for these parameters. In these extreme situations also the correlation matrix showed that the fitting parameters were very strongly correlated.

RESULTS

A typical experimental result is given in Fig. 4 where the scattering of the null matrix $^{65}Cu_{0.435}{}^{62}Ni_{0.565}$, quenched from equilibrium at 400 °C is shown. Bragg scattering could not be detected at the indicated positions. Nine shell parameters give a good fit to the experimental data. A one-parameter fit with only α_1 is clearly insufficient, especially at the smaller κ values. Similar results for a number of equilibrium states of the null matrix between 340 and 700 °C have been obtained. The composition dependence of the clustering in Cu-Ni has been investigated for a number of compositions ranging from 20 to 80 at.% Ni. Since for the given isotopes only one null matrix exists, all other compositions showed to some extent Bragg reflections and sometimes second-order reflections, depending on the composition. Some of the samples even showed multiple coherent scattering. Figure 5 shows the scattering patterns of two samples of compositions at both ends of the investigated range. Here the coherent contributions are at maximum. For all compositions, except the null matrix, the disturbance of the diffuse profile at larger κ values by these coherent contributions is so strong that only the κ region

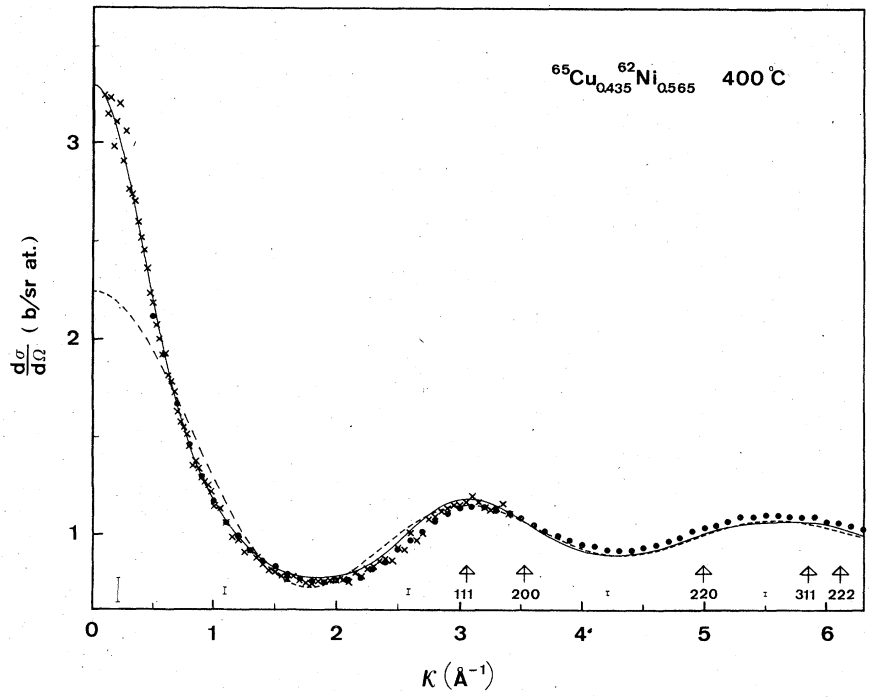

FIG. 4. Typical neutron scattering pattern: here of $^{65}Cu_{0.435}{}^{62}Ni_{0.565}$, quenched after annealing for 30 h at 400 °C. The data have been corrected only for thermal background, fast neutrons, and geometric effects in the transmission. The dashed line is a least-squares fit of Eq. (3) to the experimental points with α_1 only. The solid line a fit with α_1-α_9. The crosses were measured with 2.58-Å neutrons, the dots with 1.40-Å neutrons.

from 0.1–3.4 Å^{-1} could be used safely for an evaluation of the corresponding cluster parameters. As a consequence only the first four shell parameters have been refined for these samples. For the samples with a Ni content between 47.5 and 70 at.% the correlation range used was not quite enough for an optimal fit. Size effect parameters turned out not to be significantly different from zero, except for the three samples with highest Cu content. For all compositions equilibrium states were investigated between 400 and 700 °C. Figure 6 shows the behavior of α_{1-4} as function of the composition for most of the temperatures. For each cluster parameter the experimental error has been given also. Table II gives all cluster data with their standard deviations. In addition, as a quality factor for the fit, the ratio of the standard deviation to the statistical error averaged over all points is given. In general the quality of the fit improves by going to higher temperatures

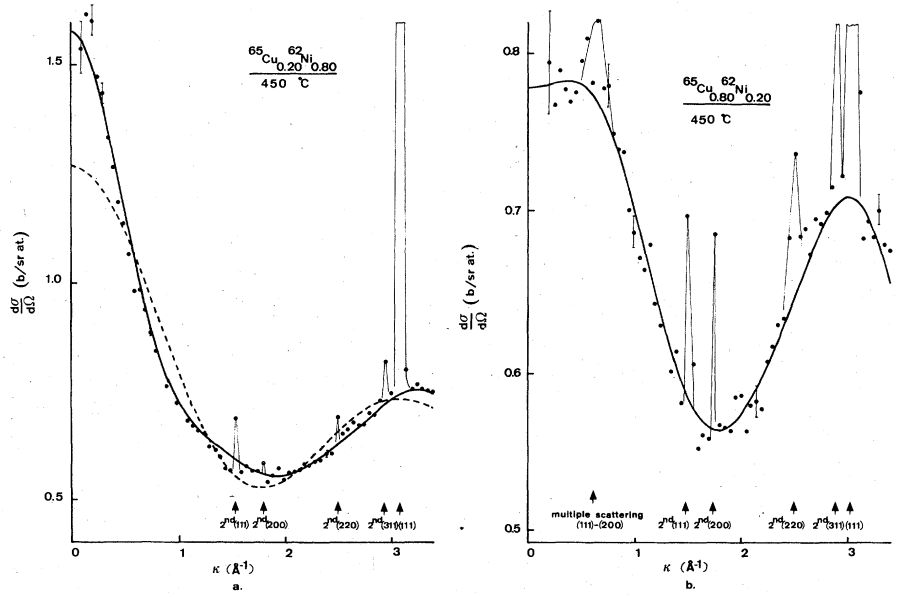

FIG. 5. Neutron-scattering patterns of $^{65}Cu_{0.20}{}^{62}Ni_{0.80}$ (a) and $^{65}Cu_{0.80}{}^{62}Ni_{0.20}$ (b), quenched from equilibrium at 450 °C and corrected similarly as in Fig. 4; $\lambda = 2.58$ Å. The solid line is a least-squares fit of Eq. (3) to the experimental data with α_1-α_4, the dashed line in (a) one with α_1 only.

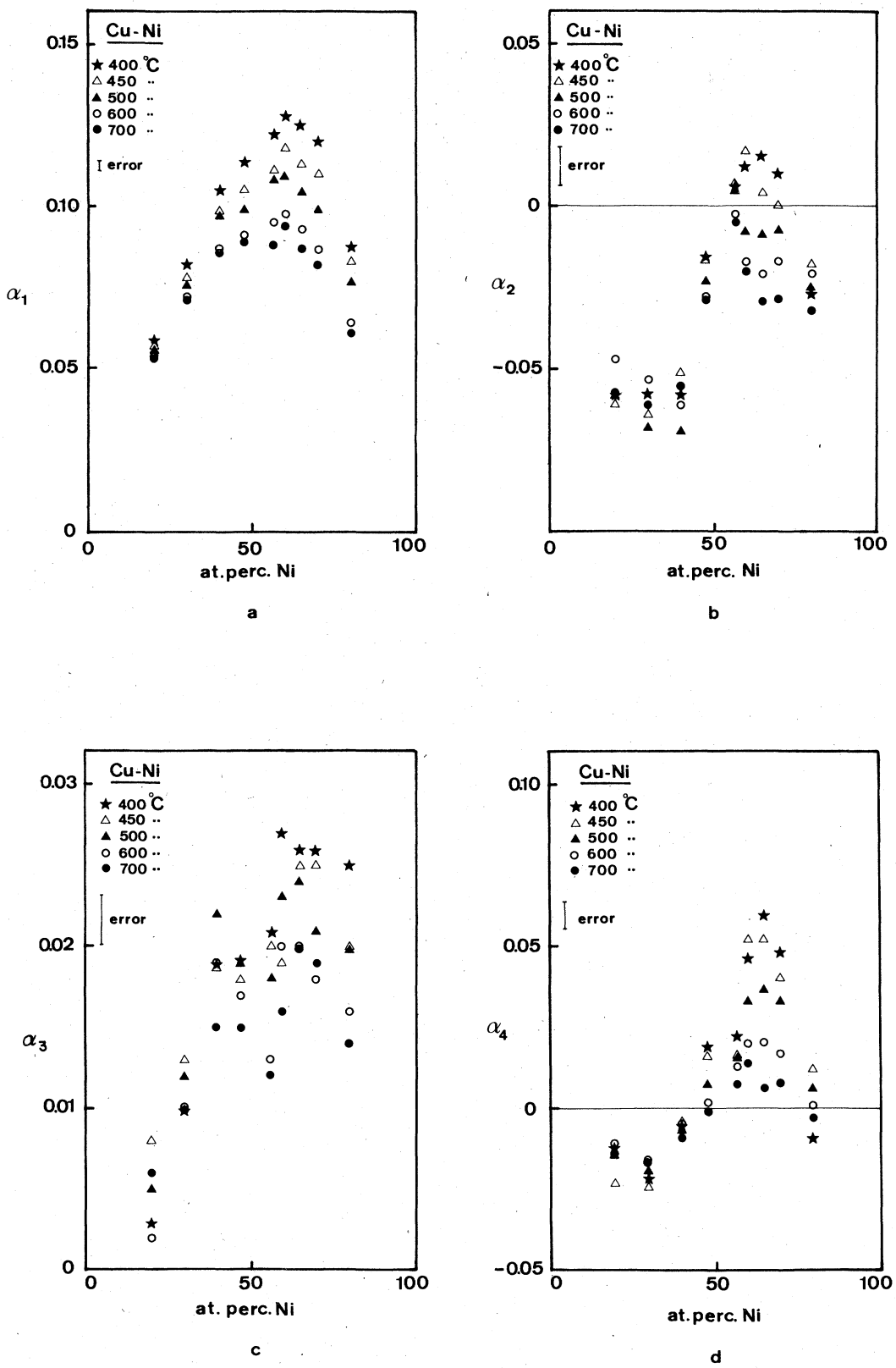

FIG. 6. Variation with temperature of the first four Warren-Cowley cluster parameters α_1-α_4 in Cu-Ni.

TABLE II. All Warren-Cowley cluster parameters for Cu-Ni from the present investigation, together with their equilibrium conditions. For a few temperatures equilibrium possibly was not established entirely. These have been marked by an asterisk. One asterisk means most probably equilibrium has not been reached entirely. Two asterisks means no equilibrium state, due to quenching from a too high temperature.

Cu-Ni	Heat treatment before quenching	α_1	α_2	α_3	α_4	st. dev.[a] / ⟨stat⟩
20-80	20 h 400 °C*	0.093(3)				4.2
		0.087(2)	−0.027(6)	0.025(2)	−0.009(4)	4.2
	40 h 450 °C	0.088(4)				9.0
		0.083(2)	−0.018(5)	0.020(2)	0.012(5)	3.0
	2 h 500 °C	0.080(3)				6.6
		0.077(1)	−0.025(5)	0.020(2)	0.006(4)	1.9
	1 h 600 °C	0.066(2)				4.9
		0.064(1)	−0.021(4)	0.016(2)	0.001(4)	1.9
	1 h 700 °C	0.060(2)				2.6
		0.061(1)	−0.032(5)	0.014(2)	−0.003(4)	1.4
30-70	60 h 400 °C	0.149(8)				20.7
		0.120(2)	0.010(7)	0.026(3)	0.048(6)	5.2
	48 h 450 °C	0.132(7)				21.5
		0.110(2)	0.000(7)	0.025(3)	0.040(6)	8.6
	2 h 500 °C	0.120(6)				10.6
		0.099(2)	−0.008(7)	0.021(3)	0.033(6)	4.0
	1 h 600 °C	0.099(4)				7.3
		0.087(2)	−0.017(6)	0.018(3)	0.017(5)	3.3
	1 h 700 °C	0.089(3)				5.4
		0.082(1)	−0.029(6)	0.019(2)	0.008(4)	2.2
	5 min 800 °C**	0.085(2)				7.8
		0.080(1)	−0.028(4)	0.019(2)	0.003(3)	3.6
	5 min 900 °C**	0.086(3)				7.3
		0.081(1)	−0.027(4)	0.019(2)	0.004(3)	2.8
	5 min 960 °C**	0.087(3)				5.1
		0.079(1)	−0.019(5)	0.017(2)	0.005(4)	2.4
35-65	60 h 400 °C	0.162(10)				32.0
		0.125(4)	0.015(9)	0.026(4)	0.059(8)	9.0
	48 h 450 °C	0.144(8)				30.4
		0.113(3)	0.004(9)	0.025(4)	0.052(8)	14.5
	2 h 500 °C	0.128(7)				24.1
		0.104(3)	−0.009(8)	0.024(4)	0.037(7)	11.1
	1 h 600 °C	0.108(4)				15.6
		0.093(2)	−0.021(7)	0.020(3)	0.021(5)	7.5
	1 h 700 °C	0.095(3)				10.7
		0.087(1)	−0.030(5)	0.020(2)	0.006(4)	5.7
80-20[b]	20 h 400 °C*	0.044(2)				5.6
		0.058(1)	−0.058(3)	0.003(1)	−0.013(2)	1.0
	40 h 450 °C	0.041(2)				3.7
		0.057(1)	−0.061(4)	0.008(2)	−0.023(3)	0.9
	2 h 500 °C	0.039(2)				3.6
		0.055(1)	−0.058(3)	0.005(1)	−0.014(2)	0.7
	1 h 600 °C	0.042(2)				4.5
		0.053(1)	−0.047(3)	0.002(1)	−0.011(2)	0.8
	1 h 700 °C	0.041(2)				4.9
		0.053(1)	−0.057(3)	0.006(1)	−0.014(2)	1.0
70-30[c]	20 h 400 °C*	0.067(2)				5.5
		0.082(2)	−0.058(5)	0.010(2)	−0.022(3)	1.9
	48 h 450 °C	0.062(2)				3.2
		0.078(1)	−0.064(4)	0.013(2)	−0.024(3)	1.1
	2 h 500 °C	0.058(2)				2.1
		0.076(1)	−0.068(4)	0.012(2)	−0.019(3)	0.8
	1 h 600 °C	0.059(1)				4.0
		0.072(1)	−0.053(4)	0.010(2)	−0.016(4)	1.5
	1 h 700 °C	0.056(2)				2.8
		0.071(1)	−0.061(6)	0.010(2)	−0.016(4)	1.0
60-40[d]	40 h 400 °C	0.101(1)				4.1
		0.105(1)	−0.058(4)	0.019(2)	−0.006(3)	1.7
	48 h 450 °C	0.096(1)				4.4
		0.098(1)	−0.051(4)	0.019(2)	−0.005(3)	2.0
	2 h 500 °C	0.091(1)				4.7
		0.097(1)	−0.069(5)	0.022(2)	−0.007(3)	1.9
	1 h 600 °C	0.081(1)				4.4
		0.086(1)	−0.061(4)	0.019(2)	−0.005(3)	2.2
	1 h 700 °C	0.079(1)				3.6
		0.086(1)	−0.056(5)	0.015(2)	−0.009(3)	2.4

TABLE II. (*Continued*)

Cu-Ni	Heat treatment before quenching	α_1	α_2	α_3	α_4	st. dev.[a] / ⟨stat⟩
40-60	144 h 375 °C*	0.178(10)				17.1
		0.134(4)	0.028(9)	0.025(4)	0.064(8)	4.6
	28 h 400 °C*	0.163(9)				22.0
		0.128(3)	0.012(8)	0.027(3)	0.046(7)	6.5
	8 h 450 °C	0.150(8)				26.6
		0.118(3)	0.017(9)	0.019(4)	0.052(8)	10.2
	6 h 500 °C	0.133(6)				20.6
		0.109(2)	−0.008(8)	0.023(3)	0.033(6)	7.7
	1 h 600 °C	0.114(4)				14.0
		0.098(2)	−0.017(6)	0.020(3)	0.020(5)	5.1
	½ h 700 °C	0.104(3)				9.7
		0.094(2)	−0.020(6)	0.016(3)	0.014(5)	3.5
52.5-47.5	144 h 375 °C	0.136(5)				7.5
		0.117(2)	−0.017(5)	0.023(2)	0.019(4)	2.0
	27 h 400 °C	0.128(4)				11.2
		0.113(2)	−0.016(5)	0.019(2)	0.019(4)	2.8
	5 h 450 °C	0.119(4)				11.1
		0.105(2)	−0.017(5)	0.018(2)	0.016(4)	3.2
	2 h 500 °C	0.108(3)				9.4
		0.098(2)	−0.023(7)	0.019(3)	0.007(4)	3.1
	1 h 600 °C	0.097(2)				6.3
		0.091(2)	−0.028(7)	0.017(3)	0.002(4)	2.3
	½ h 700 °C	0.092(2)				4.6
		0.089(1)	−0.029(5)	0.015(2)	−0.001(3)	2.0

Cu-Ni	Heat treatment before quenching	α_1	α_2	α_3	α_4	α_5	α_6	α_7	α_8	α_9	st. dev.[a] / ⟨stat⟩
43.5-56.5	500 h 340 °C*	0.136(4)									5.7
		0.142(3)	−0.012(9)	0.019(3)	0.007(7)	−0.003(4)	−0.004(12)	0.004(2)	−0.018(25)	0.002(5)	3.4
	30 h 400 °C	0.116(4)									9.4
		0.120(2)	0.005(9)	0.021(3)	0.021(9)	0.003(6)	0.001(25)	0.005(6)	−0.038(79)	0.008(10)	1.7
	8 h 425 °C	0.112(4)									7.8
		0.115(3)	0.008(10)	0.021(4)	0.018(10)	0.003(7)	0.002(30)	0.005(7)	−0.035(96)	0.006(12)	2.0
	5.3 h 450 °C	0.105(4)									8.1
		0.109(3)	0.006(10)	0.020(4)	0.015(10)	0.006(7)	−0.008(31)	0.008(7)	−0.066(100)	0.011(13)	1.6
	1 h 500 °C	0.104(3)									7.6
		0.107(2)	0.005(9)	0.018(3)	0.015(9)	0.004(6)	−0.003(24)	0.005(6)	−0.043(79)	0.009(10)	1.5
	1 h 600 °C	0.091(3)									4.6
		0.093(2)	−0.003(9)	0.013(3)	0.013(8)	0.001(6)	−0.004(25)	0.004(6)	−0.050(82)	0.008(11)	1.6
	½ h 700 °C	0.082(3)									3.3
		0.085(3)	−0.005(10)	0.012(4)	0.006(10)	0.002(7)	−0.006(32)	0.005(8)	−0.060(107)	0.008(13)	1.8

[a] st. dev., standard deviation. ⟨stat⟩, statistical error averaged over all points.
[b] $\beta_1 = 0.005(1)$, $\beta_2 = 0.003(1)$, and $\beta_3 = 0.001(1)$.
[c] $\beta_1 = 0.004(1)$, $\beta_2 = 0.002(1)$, and $\beta_3 = 0.001(1)$.
[d] $\beta_1 = 0.001(1)$.

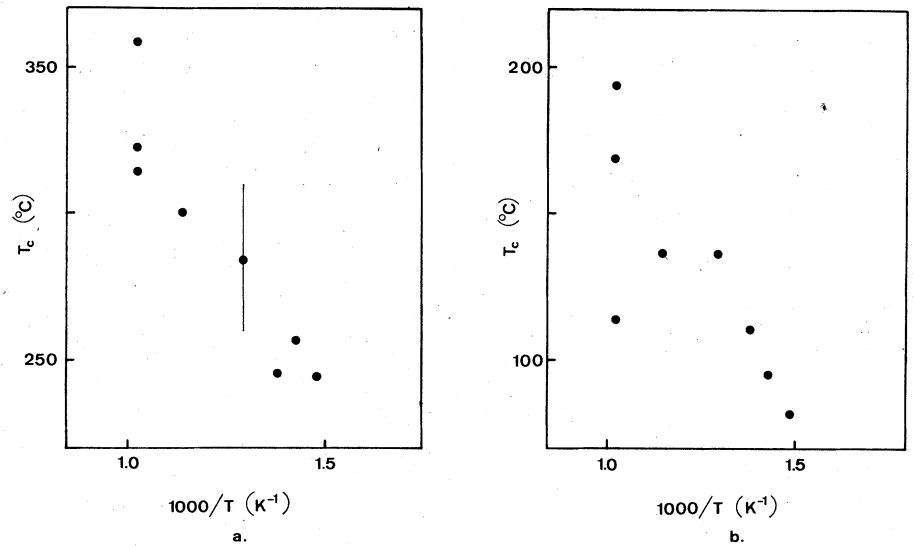

FIG. 7. T_c vs $1000/T$, calculated from the diffuse-neutron-scattering data with the model of Clapp and Moss (a) and that of Hoffman (b).

or towards the sides of the investigated composition range. This means that at lower temperatures and towards the center of the composition range the correlation range increases steadily.

Measurements of the kinetics of clustering indicated that for a few samples at the lowest temperatures the final equilibrium state possibly was not attained. These temperatures have been indicated in Table II.

DISCUSSION

Analyzing the results of the null matrix with the linear model of Clapp and Moss[8] shows a temperature dependence of the effective pairwise interaction potentials. Also the values for the critical temperature for decomposition computed from the α_i with this model depend on the temperature, as shown in Fig. 7. The same was found when the spherical model of Hoffman[10] was applied. The values for T_c calculated with the spherical model are lower than the corresponding Clapp and Moss values. These models approach the real critical temperature from opposite sites. The failure of both models in describing the temperature dependence of clustering in Cu-Ni sufficiently accurate is a first indication that in these alloys many-particle interactions might play an important role in determining the amount of clustering. This idea is supported by the results of recent computer simulations in a pairwise interaction mode,[36] which do not show this temperature dependence when analyzed with the models of Clapp and Moss or Hoffman. Furthermore, the asymmetric behavior of the cluster parameters α_{1-4} as function of the composition can not be explained by models based upon pairwise interactions like those of Clapp and Moss and of Hoffman.

Figure 8 gives the extrapolation of α_1 for T to infinity. This extrapolation is straightforward since the behavior of α_1 seems linear in $1/T$ for all compositions, as shown in Fig. 9. The slopes of these lines reflect the temperature dependence of the asymmetry of α_1 versus the composition in the investigated temperature region. For a few temperatures this is shown in more detail in Fig. 10, where it is clear that the maximum of α_1 not only increases when the temperature decreases from 700 to 400°C, but also shifts from 55 to 65 at.% Ni. This indicates a self-amplifying effect of many-particle interactions with decreasing temperature.

The distribution of the diffuse scattering intensi-

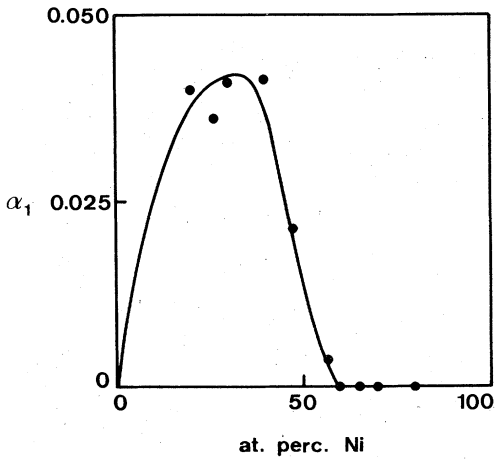

FIG. 8. Values of α_1 for $1000/T = 0$, obtained from Fig. 9, plotted vs the composition. The drawn line is a guide for the eye.

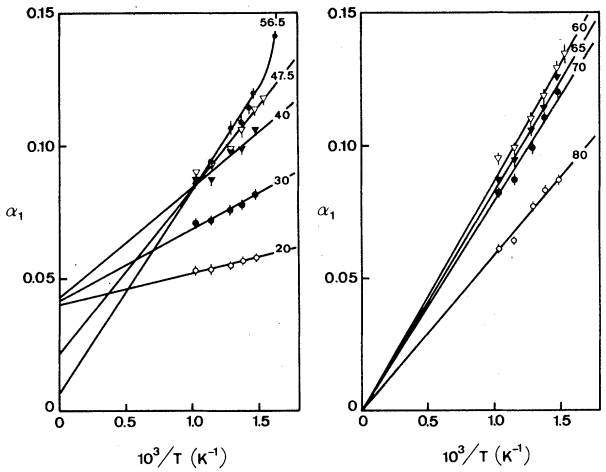

FIG. 9. Linear behavior of α_1 vs $1000/T$ for all investigated compositions in Cu-Ni. The Ni content in atomic percent is inserted in the interpolations.

ty in reciprocal space is determined by pair correlations only. This means that given a certain composition and equilibrium distribution only effective pairwise interaction potentials can be deduced from these pairwise correlations. The effect of the surroundings of a pair of atoms upon the real pairwise interactions might be deduced from the temperature and composition dependence of these effective pairwise interaction potentials. For temperatures not too close to T_c the linear model of Clapp and Moss approximates these pairwise interaction potentials very well. For the effective potentials V_1 and V_2 for first- and second-nearest neighbors, respectively, we found curves that are concave and asymmetric in the composition at the various temperatures. The absolute values for V_1 and V_2 decrease systematically with decreasing temperature.

Despite the shortcomings of the pairwise approximation, with the clustering data now available still something can be said about the shape of the miscibility gap. Figure 11 shows the predictions of the Clapp and Moss model using the pairwise interaction potentials of the various compositions. It is known that the linear model predicts T_c about 10 to 15% too high. On the other hand, relaxation experiments with the null matrix showed an initial growth of diffuse intensity at small k values at 320°C, which is probably caused by decomposition of the alloy.[26] This means that the actual values might be somewhat, but not much lower than the values computed here. Therefore the maximum of the miscibility gap is most probably located at 65-at.% Ni at a temperature between 340 and 350°C. We used the high-temperature parameters for these predictions because there the many-par-

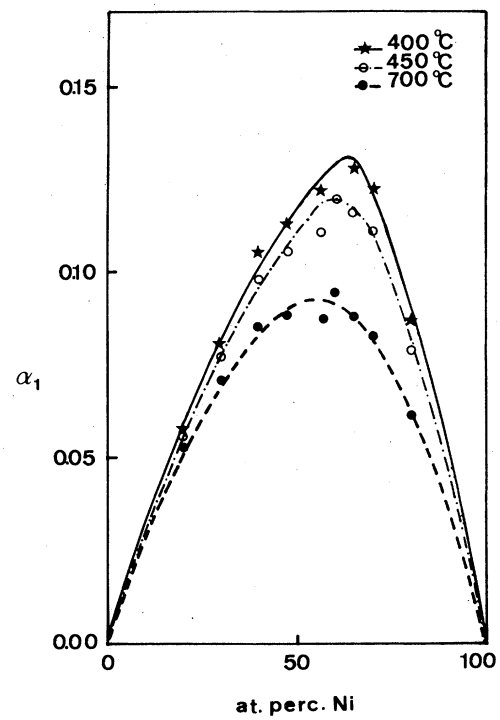

FIG. 10. First Warren-Cowley cluster parameter α_1 in Cu-Ni as a function of composition for three temperatures at which the samples were in equilibrium.

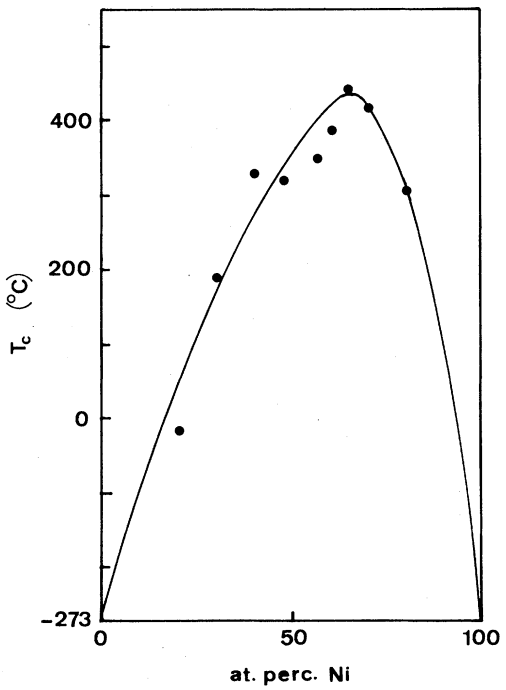

FIG. 11. Miscibility gap in Cu-Ni, calculated for the various compositions from the diffuse-neutron-scattering results with the model of Clapp and Moss. The line is drawn to guide the eye.

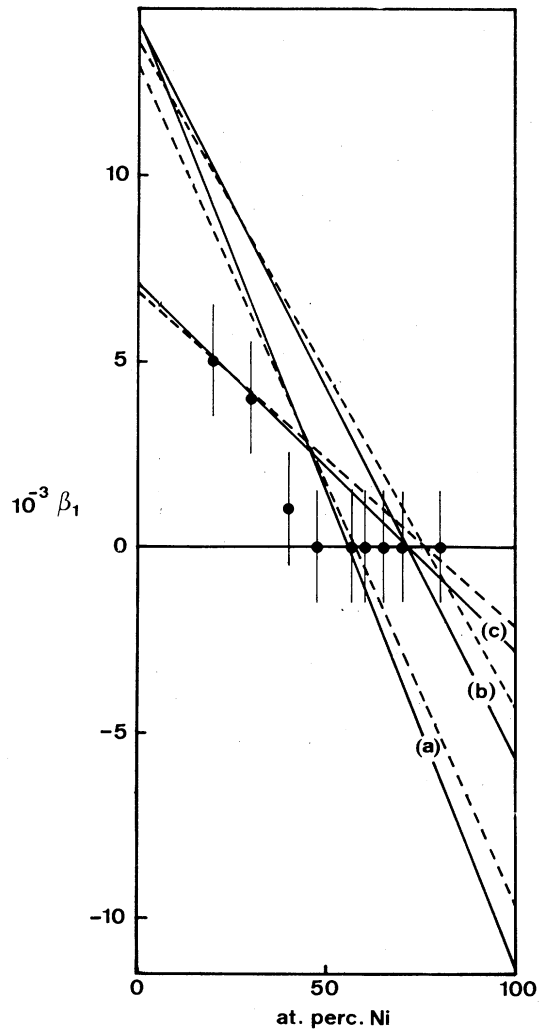

FIG. 12. Size-effect parameter β_1 for the first shell, determined experimentally as a function of the composition and calculated (a) for $\epsilon_1^{CuCu}|_{alloy} = \epsilon_1^{CuCu}|_{Cu}$ and $\epsilon_1^{NiNi}|_{alloy}$ $\epsilon_1^{NiNi}|_{Ni}$, (b) $\epsilon_1^{CuCu}|_{alloy} = \epsilon_1{}^{Cu}|_{Cu}$ and $\epsilon_1^{NiNi}|_{alloy} = \frac{1}{2}\epsilon_1^{NiNi}|_{Ni}$, and (c) $\epsilon_1^{Cu\,Cu}|_{alloy} = \frac{1}{2}\epsilon_1^{CuCu}|_{Cu}$ and $\epsilon_1^{NiNi}|_{alloy} = \frac{1}{4}\epsilon_1^{NiNi}|_{Ni}$. All calculations have also been made taking into account clustering ($\alpha_1 = 0.09$). These are given by the dotted lines.

ticle effects are minimal. Despite the scatter in the points and the possible systematic errors due to the model that was used the location of the maximum and the shape of the curve for T_c versus composition are much more detailed than the predictions for $T_{c,max}$ reported so far in the literature. These were based upon various different observations and ranged from 50 to 80 at.% Ni at temperatures between 100 and 650 °C. For diffusion with thermal vacancies only this region of the phase diagram is inaccessible in practice. Since interstitials are mobile down to much lower temperatures,[37,38] irradiation-enhanced diffusion may be applied to obtain information about the exact location of the miscibility gap.

With assumptions for the relaxation of the distance between two atoms when one of them is replaced by an atom of the other kind, size effect parameters can be calculated. Figure 12 shows the results for β_1 for various assumptions of ϵ_1^{NiNi} and ϵ_1^{CuCu}. The first is that the Cu-Cu and the Ni-Ni distances are the same as in the pure elements. A second is that a Ni-Ni pair will adapt its distance to the change in lattice parameter more easily than a Cu-Cu pair. Therefore, it was assumed that $\epsilon_{1,alloy}^{NiNi} = 0.5\,\epsilon_{1,pure\ Ni}^{NiNi}$. Furthermore both assumptions were modified by taking into account a reasonable and for computational convenience constant amount of clustering ($\alpha_1 = 0.09$) for all compositions. This still results in deviations from the values experimentally found for β_1. Relaxing the relative displacements of the last assumption both for Cu-Cu and for Ni-Ni with 50% gives a reasonable agreement. Reality will be more complex, but it may be concluded that the lattice distortions in Cu-Ni are very small indeed, even smaller than expected from the 3% difference in lattice parameters of the pure elements. Consequently, elastic strain due to clustering also will be very small.

It seems worthwhile to compare the present results to those of other neutron experiments, collected in Table I. However, only the data of Mozer *et al.* appear to be comparable with those of our 47.5-at.% Ni sample, except that their value for α_1 (= 0.121) is too large for the 550 °C state they claimed. Considering clustering kinetics as derived from the relaxation of the electrical resistivity by Van Royen *et al.*[30] shows that the average relaxation time amounts roughly to 50 sec at 450 °C instead of at 550 °C, as was derived from tracer diffusion data for Ni,[40] by Mozer *et al.* This agrees even better with our data. However, it must be emphasized once again that in *none* of the other investigations equilibrium states were measured.

SUMMARY AND CONCLUSIONS

A detailed set of cluster parameters has been obtained which describes the equilibrium distribution of the atoms in Cu-Ni as a function of temperature and composition. The temperature dependence cannot be described sufficiently accurately by pairwise interaction models. The clustering parameters are asymmetric in the composition. Also this asymmetry appears to be temperature dependent. Consequently many-particle interactions play an important role in determining the amount of clustering in Cu-Ni. Size effects are

smaller than expected. The parameters of Table II can be of great help in understanding the nature and extent of these many-particle interactions. From these data the shape of the miscibility gap and the location of its maximum have been constructed. The detailed knowledge of clustering in Cu-Ni can also be used as a probe to investigate physical phenomena which are influenced by local environmental effects. An example of this is a recent investigation of the effect of clustering upon the behavior of the magnetic moment of Ni atoms in Cu-Ni alloys, which was based upon the knowledge of the different clustered states of the samples.[39]

ACKNOWLEDGMENTS

We wish to thank Dr. D. W. Hoffman for his interest in this work and for his model calculations, Dr. C. van Dijk for his stimulating discussions, H. J. Bron of the Laboratorium voor Fysische Metaalkunde, Groningen University, for his assistance in preparing the specimen, Dr. Th.H. de Keijzer of the Laboratorium voor Metaalkunde, Technical University of Delft, for his texture analysis, and W. van der Gaauw for his technical assistance in the experiments. The FOM (Stichting Fundamenteel Onderzoek der Materie) sponsored this work with a grant for the isotopes.

[1]S. C. Moss, J. Appl. Phys. 35, 3547 (1964).
[2]D. H. Wu and R. A. Tahir-Kheli, J. Phys. Soc. Jpn. 31, 641 (1971).
[3]P. Bardhan and J. B. Cohen, Acta Crystallogr. Suppl. A 31, 186 (1975).
[4]E. Metcalfe and J.A. Leake, Acta Metall. 23, 1135 (1975).
[5]S. Radelaar, thesis (Delft, 1967) (unpublished).
[6]F. Zernike, Physics 7, 565 (1940).
[7]J. M. Cowley, Phys. Rev. 77, 669 (1950); 120, 1648 (1960); 138, A1384 (1965).
[8]P. C. Clapp and S. C. Moss, Phys. Rev. 142, 418 (1966); 171, 754 (1968); S. C. Moss and P. C. Clapp, *ibid.* 171, 764 (1968).
[9]R. A. Tahir-Kheli, Phys. Rev. 188, 1142 (1969).
[10]D. W. Hoffman, Met. Trans. 3, 3231 (1972).
[11]R. Kikuchi, Phys. Rev. 81, 988 (1951).
[12]C. M. van Baal, Physica 64, 571 (1973).
[13]J. L. Meijering, Acta Metall. 5, 257 (1957).
[14]W. Köster and W. Schüle, Z. Metallkd. 48, 592 (1957).
[15]R. A. Oriani and W. K. Murphy, Acta Metall. 8, 23 (1960).
[16]R. A. Rapp and F. Maak, Acta Metall. 10, 63 (1962).
[17]B. N. Dey, Scr. Metall. 2, 501 (1968); J. Appl. Phys. 35, 3621 (1964).
[18]A. Kidron, Phys. Lett. 26A, 593 (1968); Phys. Rev. Lett. 22, 774 (1969).
[19]F. M. Ryan, E. W. Pugh, and R. Smoluchowski, Phys. Rev. 116, 1106 (1959).
[20]M. F. Ebel, Phys. Status Solidi A 5, 91 (1971).
[21]B. Mozer, D. T. Keating, and S. C. Moss, Phys. Rev. 175, 868 (1968).
[22]J. W. Cable, E. O. Wollan, and H. R. Child, Phys. Rev. Lett. 22, 1256 (1969).
[23]A. T. Aldred, B. D. Rainford, T. J. Hicks, and J. S. Kouvel, Phys. Rev. B 7, 218 (1973).
[24]R. A. Medina and J. W. Cable, Phys. Rev. B 15, 1539 (1977).
[25]P. de Gasperis, F. Dupré, and J. I. Budnick, J. Magn. Magn. Mat. 1, 289 (1976).
[26]J. Vrijen and C. van Dijk, in *Fluctuations, Instabilities and Phase Transitions*, edited by T. Riste (Plenum, New York, 1975).
[27]B. E. Warren, *X-Ray Diffraction* (Addison-Wesley, Reading, Mass., 1969).
[28]J. Bergsma and C. van Dijk, Nucl. Instrum. Meth. 51, 121 (1967).
[29]J. Andries, W. G. Boon, and S. Radelaar, Phys. Lett. 38A, 459 (1972).
[30]E. W. van Royen, G. Brandsma, A. L. Mulder, and S. Radelaar, Scr. Metall. 7, 1125 (1973).
[31]G. Placzek, Phys. Rev. 86, 377 (1952); 93, 895 (1954); 105, 1240 (1957).
[32]J. L. Yarnell, M. J. Katz, R. G. Wenzel, and S. H. Koenig, Phys. Rev. A 7, 2130 (1973).
[33]G. H. Vineyard, Phys. Rev. 96, 93 (1954).
[34]V. F. Sears, Adv. Phys. 24, 1 (1975).
[35]S. F. Mughabghab and D. I. Garber, *Neutron Cross Sections*, 3rd ed. *Resonance Parameters*, Brookhaven report No. BNL-325, 1973 (unpublished), Vol. 1.
[36]E. W. van Royen, J. Vrijen, and S. Radelaar (unpublished).
[37]R. Poerschke, thesis (Aachen, 1974) (unpublished).
[38]R. Poerschke and H. Wollenberger, J. Phys. F 6, 27 (1976).
[39]C. van Dijk and J. Vrijen, J. Magn. Magn. Mat. (to be published).
[40]K. Monma, H. Suto, and H. Oikawa, J. Jpn. Inst. Met. 28, 192 (1964).